A Kinetic Model for the Glycosidation of D-glucose and n-decanol

N. S. Chaubal, V. Y. Joshi, and M. R. Sawant
Department of Chemistry, Institute of Chemical Technology (Autonomous)
University of Mumbai, Matunga, Mumbai – 400 019. India

Original scientific paper
Received: October 2, 2006
Accepted: March 1, 2007

Kinetics of the acid catalyzed glycosidation reaction has been investigated over a broad range of operating conditions. The effect of mass transfer, speed of agitation, catalyst loading, substrate concentration, and temperature on the reactions has been reported. The effects of various solvents on the reaction have been investigated. A glycosidation reaction was found to be zero order with respect to the n-decanol concentration. The experimental data could be fitted into the model involving a surface reaction controlling mechanism with dissociative adsorption of n-decanol and D-glucose for glycosylation reaction. The apparent activation energy for the catalytic glycosidation of D-glucose was found to be 36.75 kJ mol^{-1}.

Key words:
Kinetic modelling, glycosidation, D-glucose, n-decanol, heterogeneous acid catalyst.

Introduction

Carbohydrates possess a higher density of functional groups than any other class of compounds. Interactions between these groups and competing reactions between different groups occur frequently; hence, this is a rich field for the study of complex reaction mechanism.[1] A number of glycosides and oligosaccharides are found in many bioactive functional molecules. One of the most important transformation reactions of carbohydrates is a chemical glycosidation, which is very useful for preparing both natural and synthetic glycosides.[2] Therefore, a highly effective, simple and environmentally benign glycosidation method is urgently needed both in the laboratory and in industry. In this context, the chemical glycosylation may include the use of a heterogeneous and reusable mixed metal solid acid as an activator. Glycosidation of simple alcohols with D-glucose can be performed by strong acids like HF,[3] BF_3-etherate,[4] HCl,[5] para toluene sulphonic acid and H_2SO_4[6] to give both α and β-anomers with high degree of polymerization of glucose unit. Such glycosidation normally proceeds in moderate yield (40–50 %). *Toshima*[7] used montmorillonite K-10 as a heterogeneous solid catalyst for glycosidation of olivoses. Later on, same research group used montmorillonite K-10 with benzyl-protected glucopyranosyl phosphate and several alcohols to get β-*O*-glycosidic linkages in more than 80 % yield.[8] In our previous studies,[9] we have demonstrated stereoselective β-D-glucopyranosylation of 2,3,4,6-tetra-*O*-acetyl--α-D-glucosylbromide and fatty alcohols over $LiCO_3$ as reaction promoter. Such reaction promoter has limited activity and catalytic life. Highly effective and recyclable glycosidation methods without protection and halogenations have attracted our attention. Therefore we studied glycosidation reactions of n-decanol with D-glucose using various experimental conditions to understand reaction kinetic and probable reaction mechanism over w = 10 % of $ZnFe_2O_4$ on ZrO_2. The advantages of w = 10 % of $ZnFe_2O_4$ on ZrO_2 in glycosidation reaction is described in detail eleswhere.[10] Though number of synthetic routes for glycosidation are reported in the literature no attempts to study the kinetics of the glycosidation reaction of D-glucose and n-decanol over solid catalysts has been made. Hence, our objective is to study the kinetics and modelling using the regression of experimental results of the glycosidation reaction over solid catalysts in order to understand the detail pathways followed by the reaction over the heterogeneous catalyst surface to selectively produce β anomer.

Experimental

Materials and chemicals

Nitrates of zinc, iron and zirconium oxychloride of analytical reagent were used for catalyst preparation. D-glucose and n-decanol of analytical grade were used with out further purification. The catalyst was prepared by template route. All the solvents such as toluene, acetic acid, dimethylformamide and tetrahydrofuran used are of analytical grade.

All the materials and chemical used in the glycosidation reaction were obtained from ms. s.d. fine-chem. Ltd.

Synthesis of catalyst

Templated approach[10]

In a typical preparation, Fe and Zn nitrates were taken in, stoichiometric amounts $r_{Fe/Zn} = 2 : 1$ and were dissolved in 10 ml of methanol to this 10 ml of decyl polyglycoside (50 %) aqueous solution was added with vigorous stirring for 1h. The resulting solution was gelled at 50 °C for 20 h (catalyst preparation is optimized). Similarly, $ZrOCl_2 \cdot 7H_2O$ was treated with decyl polyglycoside (50 %) aqueous solution and gelled at 50 °C for 20 h. Both, Fe + Zn and Zr gels were mixed together aged for 5 h, dried at 100 °C. This as made bulk sample was calcined at 900 °C for 9 h in air to remove the surfactant to obtain $w = 10$ % of $ZnFe_2O_4$ on ZrO_2. The catalyst is characterized in detail using various characterization techniques.

Characterization of $w = 10$ % of $ZnFe_2O_4$ on ZrO_2

Catalysts were characterized by X-ray diffraction, BET surface area measurement, FT-IR measurement.

Reaction methodology and product analysis

The reactor consisted of a standard flat bottom cylindrical vessel of 5 cm i.e. of 100 ml capacity equipped with four equi-spaced baffles, a pitched-bladed turbine impeller and a condenser. The assembly was kept in an isothermal oil bath at a known temperature and mechanically agitated with an electric motor. Melting points were determined using capillary method. Specific rotations were recorded on a manual polarimeter. Infra red spectroscopy was recorded on model 500 spectrophotometer, Buck scientific inc. ^1H NMR were recorded on model of Hitachi inc. and operated at 300 MHz. All the data are uncorrected. $w = 10$ % of $ZnFe_2O_4$ on ZrO_2 was studied for its catalytic behaviour towards glycosidic bond formation with n-decanol at the 363 K. In a typical reaction D-glucose (10 mmol) in toluene (16 ml) was stirred for fifteen minutes at room temperature. Then $w = 10$ % of $ZnFe_2O_4/ZrO_2$ catalyst (8.8 mg cm^{-3}) and n-decanol (30 mmol) was add, the reaction carried at 363 K for stipulated time. Reaction mass was cooled and filtered over celite. Filtrate was evaporated in vacuum and the resulting material was purified by column chromatography ($\Psi_{\text{toluene/ethyl acetate}} = 15 : 5$) to afford poly β-D-glucopyranoside.

Variety of solvents was used for the glycosidation reaction. From electronic energy of solvents it was observed, as electronic energy decrease from toluene (–4350.85 eV) > THF (–3472.47 eV) ≈ DMF (–3411.05 eV) > DMSO (–2544.99 eV) ≈ acetic acid (–2535.6 eV) increases the formation of polyglucose by suppressing the formation of β-D-glucopyranoside. As the reaction follows LHHW model 3 where the formation of β-D-glucopyranoside was more in toluene and product obtained was yellowish with degree of polymerization in desirable range, also the solvent recovery was easy. All further reactions were taken in toluene as reaction media.

Results and discussions

XRD of $ZnFe_2O_4/ZrO_2$ prepared by template method indicates amorphous nature of the catalyst. BET specific surface area is 180 m^2 g^{-1}. Due to the amorphous nature of $ZnFe_2O_4/ZrO_2$ the nanocrystallite size cannot be determined. Pore diameter and measurement of $ZnFe_2O_4/ZrO_2$ is very high; 3.0 nm due to template assisted route. Oxidic spinel generally shows four IR active fundamentals in the vibrational spectra (Fig. 1). The two high frequency bands are broad and tend to be asymmetric due to condensed octahedra, while low frequency bands are weak and are due to displacement of tetrahedral cation. In $ZnFe_2O_4$ the high frequency bands at 576 due to Fe-O stretching and 686 cm^{-1} due to Zn–O stretching, were observed merged as a broad band. In $ZnFe_2O_4/ZrO_2$ the single broad band is observed at 381–717 cm^{-1}. This may be attributed to the effect of zirconia, which shows the broad band in the region of 349–727 cm^{-1}. It is obvious from the above observation that the stretching frequency depends upon the cation distribution between the tetrahedral and octahedral sites. Modification in the vibration frequency may arise due to simultaneous changes in quantities such as cationic mass, the cation/oxygen distance, binding force and unit cell dimensions.[11] It is not possible to distinguish between relative contributions of these different factors at this stage. Pyridine adsorbed FT-IR of $ZnFe_2O_4/ZrO_2$

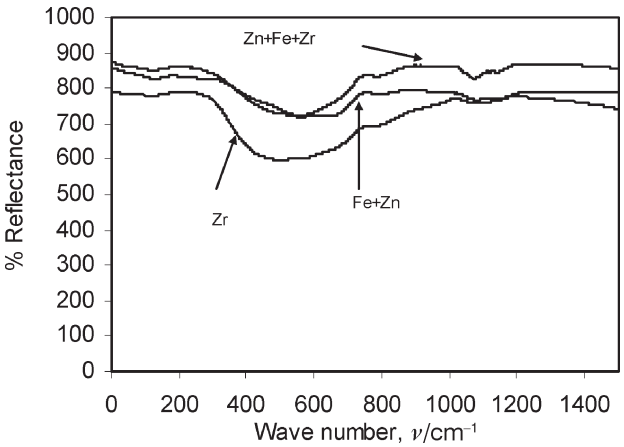

Fig. 1 – *DRIFT spectra*

the bands observed at ~1635, ~1493 and ~1541 cm^{-1} are assigned to pyridine molecules bound to Brönsted acid sites and shows peaks at ~1612, ~1490, and ~1448 cm^{-1} that are due to pyridine molecules bound to Lewis acid sites. It was thought desirable to study various reaction quantities under otherwise similar experimental conditions to establish the reaction kinetics and modelling.

Mass transfer considerations

As shown in the Fig. 2, glycosidation is typical solid liquid slurry reaction involving the transfer of D-Glucose (A) and n-decanol (B) to the catalyst wherein external mass transfer of the reactants to the surface of the catalyst particle, followed by intraparticle diffusion, adsorption, surface reactions and desorption takes place. (C) is the main product called decyl glucoside while (D) is the major by-product called polyglucose. Following assumptions were made while studying the kinetics of glycosidation,

1. The activity of the catalyst is maintained throughout in all the experiment, that is, no

poisoning or deactivation of the catalyst occurs.

2. Desorption of the products offered no resistance[12]

For the purpose of kinetic study, it is important to ensure that the rate data are obtained under the kinetically controlled regime. Thus experimental and theoretical analyses were done. The reaction studied involves two reactants in organic phase, which reacts on the surface of the catalyst to form liquid phase products at the reaction temperature chosen. As n-decanol was always used in excess, there is likelihood of mass transfer resistance to the transfer of D-glucose from the bulk liquid phase to the external surface of catalyst particle. Applying steady state approximation, the rate of mass transfer per unit volume of the liquid phase is,

Rate of transfer of A from bulk liquid to external surface on the catalyst particle

$$r_A = k_{SL\text{-}A}\, a_p\{[A_O] - [A_S]\} \quad (1)$$

Rate of transfer of B from bulk liquid to external surface on the catalyst particle

$$r_B = k_{SL\text{-}B}\, a_p\, \{[B_O] - [B_S]\} \quad (2)$$

$$= r_{obs} \quad (3)$$

= rate of reaction with in the catalyst particle

Where, k_{SL} is the solid-liquid mass-transfer coefficient of the concerned species (cm s^{-1}), a_p is the external surface area of the particle (cm^2 cm^{-3} liquid-phase volumic area), subscript $_O$ and $_S$ denote the bulk liquid phase and external surface concentrations respectively, in mol cm^{-3}. Eq. (3) could be represented by a Langmuir-Hinshelwood-Hougen-Watson type, power law model or Eley-Rideal model with or without the effectiveness factor η to account for the intraparticle diffusion resistance. It was seen that depending on the relative magnitudes of external resistance to mass transfer and reaction rates, different controlling mechanisms have been put forth. When the external mass-transfer resistance is small, then the following inequality holds,

$$1/R_{obs} >> \frac{1}{k_{SL-A}\,ap[Ao]} \text{ and } \frac{1}{k_{SL-B}ap[Bo]} \quad (4)$$

It is therefore necessary to study the different effects like speed of agitation, temperature, effect of catalyst loading, solvent effect etc to ascertain the absence of external and intraparticle resistance so that a true intrinsic kinetic equation could be used. The selection of the reaction mechanism was based on the following criteria,

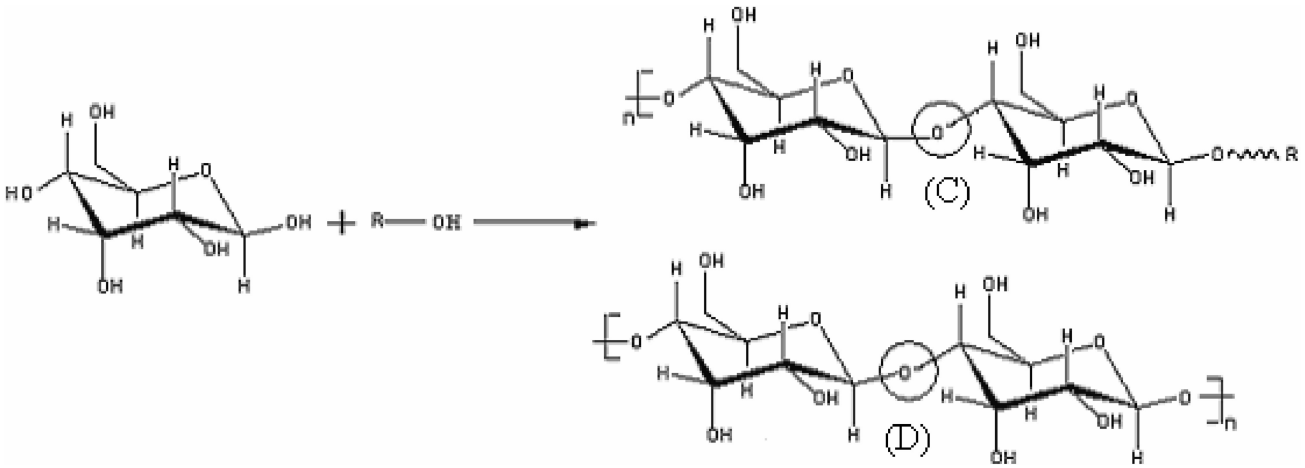

Fig. 2 – *Glycosidation of D-glucose using n-decanol*

(a) That all the coefficients must be positive and significantly different from zero

(b) That the reaction velocity constant and adsorption equilibrium constant must be temperature-dependent

(c) If more than one mechanism satisfied the conditions given above, then whichever mechanism gives the best fit between experimental and calculated reaction rates was selected as the correct mechanism.

In the glycosylation reactions, liquid-liquid, liquid-solid and intraparticle diffusion (pore diffusion) resistances are likely to be important for consumption of n-decanol. A very direct test of the importance of liquid-liquid and liquid-solid transport was made by running the several experiments at different agitation speeds, with all other variables constant. The initial rate was found to increase significantly when the speed increases from n = 600–1500 min, but it remained constant after n = 900 min^{-1} for the glycosylation reactions. It appears from these results that the resistance to liquid-liquid/liquid-solid mass transfer is not significant. Theoretical analysis was also done to ensure that the external mass-transfer resistance was indeed absent. According to eq. 3, it is necessary to calculate the rates of external mass transfer of both D-glucose (A) and n-decanol (B) compared them with the rate of reaction. For a typical spherical particle, the particle surface area per unit liquid volume is given by

$$a_p = \frac{6\gamma}{\rho_p d_p} \tag{5}$$

Where γ = catalyst loading g cm^{-3} of liquid phase, ρ_p = density of particle g cm^{-3} and d_p = particle diameter in cm. The maximum catalyst loading used (0.01 g cm^{-3}), d_p = 0.9 cm, in the current studies a_p = 6.67 cm^{-1}. The liquid-phase diffusivity values of the reactants A and B, denoted by D_{AB} and D_{BA}, were calculated by using the *Wilke-Chang*[13] equation at 363 K as 6.15 · 10^{-4} and 1.64 · 10^{-4} cm^2 s^{-1}, respectively. The solid-liquid mass transfer coefficient for both A and B were calculated from the limiting value of the Sherwood numbers[14] of 2. The actual Sherwood numbers are typically higher by order of magnitude in well-agitated systems but for conservative estimations a value of 2 is taken. The solid-liquid mass-transfer coefficients $k_{SL\text{-}A}$ and $k_{SL\text{-}B}$ values were obtained as 1.37 · 10^{-3} and 3.65 · 10^{-3} cm s^{-1}, respectively. The initial rate of reaction was calculated from the conversion profiles. A typical calculation shows that for a typical initial rate of reaction was calculated as1.58 · 10^{-6} mol cm^{-3} s^{-1}. Therefore, putting the appropriate values in eq. 4 the respective values are,

$$6.33 \cdot 10^5 >> 1.09 \cdot 10^4 \text{ and } 2.05 \cdot 10^3$$

The above inequality demonstrates that there is an absence of resistance due to the solid-liquid external mass transfer for both the species A and B and the rate may be either surface-reaction-controlled or intraparticle-diffusion-controlled. This also supported the theoretical calculations for further proof of the absence of the intraparticle- diffusion- resistance was obtained through the study of the effect of temperature.

Analysis of experimental initial rate data

The effects of catalyst loading and temperature on the experimental initial rate of reactions are shown in Fig. 3 and 4. The rate was found to increase linearly with the catalyst loading and temperature for both the reactions. From the effect of catalyst concentration on initial rate of reaction, the order of the reaction was obtained. The reaction order with respect to n-decanol was obtained by regression analysis at different temperatures and catalyst loadings. The reaction was zero order with re-

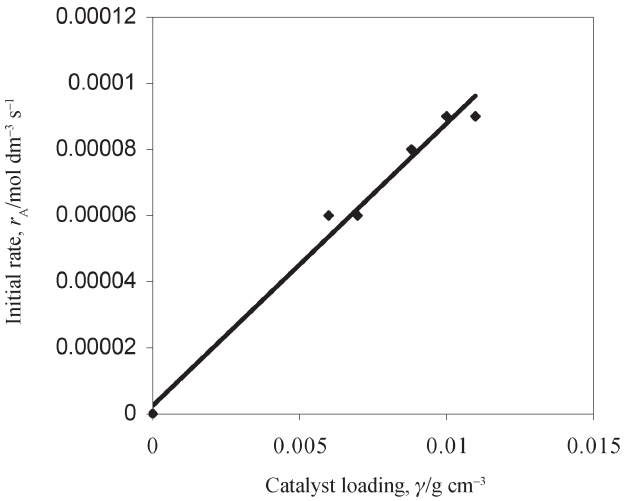

Fig. 3 – *Initial rates vs. catalyst loading*

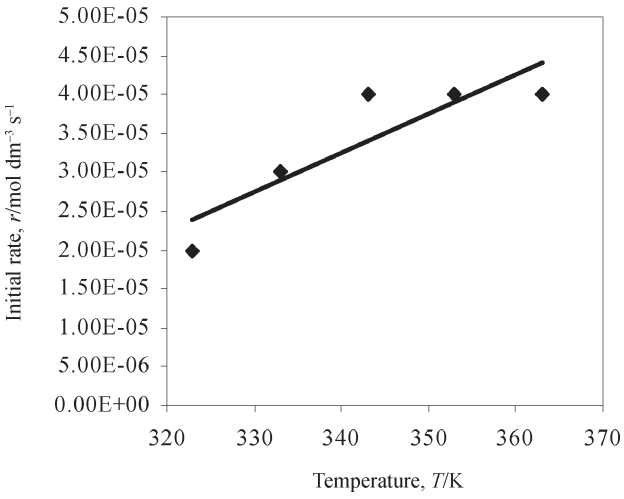

Fig. 4 – *Initial rates vs. temperature*

spect to catalyst loading. It was found that reaction temperature had a strong effect on the initial rate of the reactions. The initial rates were found to increase with increasing the reaction temperature for the reaction.

Kinetic model

In the present study, the rate data has been analyzed by non-linear least square method of analysis through a computer program (graph pad prism version 4.0). The selection of the reaction mechanism was based on the following criteria (a) That all the coefficients must be positive and significantly different from zero (b) That the reaction velocity constant and adsorption equilibrium constant must be temperature dependent (c) If more than one mechanism satisfied the conditions given above, then whichever mechanism gives the best fit between experimental and calculated reaction rates was selected as the correct mechanism.

A Langmuir-Hinshelwood (L-H) type model has been proposed to describe both the reactions. Several variations of the L-H model (Table 1) were evaluated. For glycosidation of D-glucose, estimated parameters (Table 2 & 3) for all models (except model 1, 3, 4, 5 and 6) were negative and hence these models were not considered. A comparison of the residual sum of square or the variance or correlation coefficient of the five models at all temperatures indicates that model 3 based on surface reaction controlling of molecularly adsorbed n-decanol is the best model as compared to model 4 and 6. The agreement between the model predictions and the experimental results (Fig. 5) was excellent, indicating that the model 3 is the best model for representing the kinetics of glycosidation of D-glucose.

The Arrhenius plot of $1/T$x 1000 *vs.* ln (k) (Fig. 6) gave the apparent activation energy to be 36.75 kJ mol^{-1} by the equation $-E_a$ = slope/R, where R = 8.314 J mol^{-1}. Normally, a reaction that is controlled by external mass transport (either gas-liquid

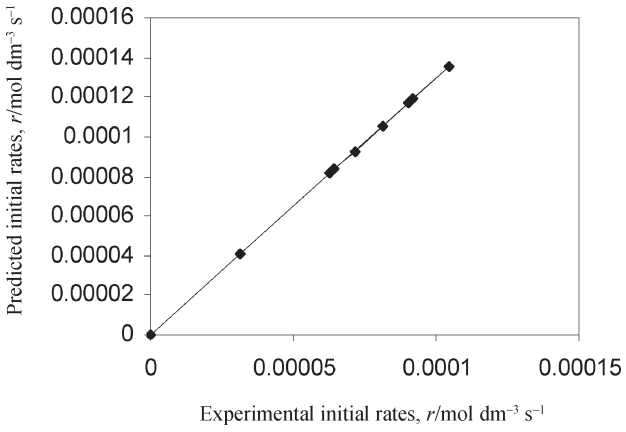

Fig. 5 – *Predicted rates vs. experimental initial rates*

Table 1 – *L-H models for the different controlling mechanism*

Models	Equation
Single site-molecularly adsorbed D-glucose and molecularly adsorbed n-Decanol	
1	$r = K_1 \cdot c_A / (1 + K_B \cdot c_B)$
2	$r = K_1 \cdot c_A / (1 + K_c \cdot c_B)$
3	$r = (K_1 \cdot K_B \cdot K_c \cdot c_A \cdot c_B) / (1 + K_c \cdot c_A + K_B \cdot c_B)^2$
Single site-molecularly adsorbed D-glucose and atomically adsorbed n-Decanol	
4	$r = (K_1 \cdot c_A) / (1 + (K_B \cdot c_B)^{0.5}$
5	$r = (K_1 \cdot c_B) / (1 + K_c \cdot c_A)^2$
6	$r = (K_1 \cdot K_c \cdot K_B \cdot c_A \cdot c_B) / (1 + K_c \cdot c_A + (K_B \cdot c_B)^{0.5})^3$
Single site-molecularly adsorbed D-glucose and n-decanol in the liquid-phase	
7	$r = (K_1 \cdot K_c \cdot c_A \cdot c_B) / (1 + K_c \cdot c_A)$
Dual site-molecularly adsorbed D-glucose and molecularly adsorbed n-decanol	
8	$r = (K_1 \cdot K_c \cdot K_B \cdot c_A \cdot c_B) / (1 + K_c \cdot c_A) \cdot (1 + K_B \cdot c_B)$
Dual site-molecularly adsorbed D-glucose and atomically adsorbed n-decanol	
9	$r = (K_1 \cdot K_c \cdot K_B \cdot c_A \cdot c_B) / (1 + K_c \cdot c_A) \cdot (1 + K_B \cdot c_B)^2$

Table 2 – *Second order polynomial coefficients at 363 K*

Catalyst loading γ/mg cm^{-3}	6.0	7.0	8.8	10.0	11.0
A	–0.00107	–0.00129	–0.00150	–0.00179	–0.00172
B	8.94e–5	10.82e–5	13.36e–5	15.98e–5	15.85e–5
C	–1.385e–7	–1.870e–7	–2.560e–7	–3.246e–7	–3.211e–7

Table 3 – *Parameters of L-H models at 363 K*

Model	Catalyst loading at γ/8.8 mg cm^{-3}		
	K_1	K_B	K_C
1	0.06513	7.22E-5	–
3	1764	2277	3.10E6
4	14.46	1.076	–
5	2.913	91.73	–
6	13	11.14	13.01

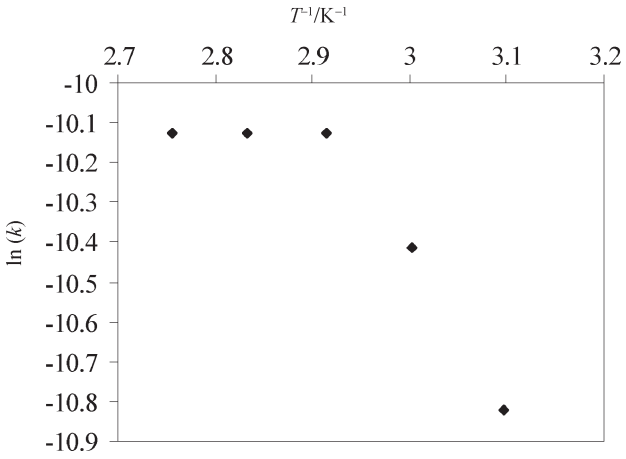

Fig. 6 – *Arrhenius plot*

or liquid-solid mass transport) has activation energy of less than about 25 kJ mol^{-1}.[15] Therefore, these high values of observed activation energies suggest that the influence of both gas-liquid and liquid-solid mass transport was negligible in this study.

Reaction and reaction mechanism

The β-glycosidic bond formation of D-glucose with alcohol is one-step reaction as shown in Fig. 7 below (*see glycosidic bond formation in the circle*). In the reaction (C) is the major product whereas (D) is side product. Formation of (D) alters the physico-chemical property of polyglycoside so product (D) is undesirable, hence, the reaction suffers and application of the product is restricted. $ZnFe_2O_4$/ ZrO_2 possess electron rich and electron deficient sites (i.e. negative and positive respectively) on the surface.

The mechanism of glycosidation was correlated with L-H model 3, in which aldoses or ketones on treatment with alcohols containing acid catalysts yield glycosides as a major product. The major reaction takes place usually via α-furanoside or β-furanoside formation. Such intermediates further convert to pyranosides. For present catalytic system we suggest following mechanism where both the substrate, are molecularly adsorbed on catalytic surface so ring opening approach is more suitable than neighbouring group participation. As D-glucose (A) shows anomerization of pyranose form which presumably is occurring rapidly under acidic conditions.[17] This anomerization occurs via ring opening followed by addition of fatty alcohol (B) to form unstable intermediate (C) and lost of water molecule to form α-furanoside or β-furanoside (D). Presently we are not sure about the exact anomeric form of furanoside; however, the major product is alkyl poly β-D-glucopyranoside. Another alcohol molecule addition and elimination in

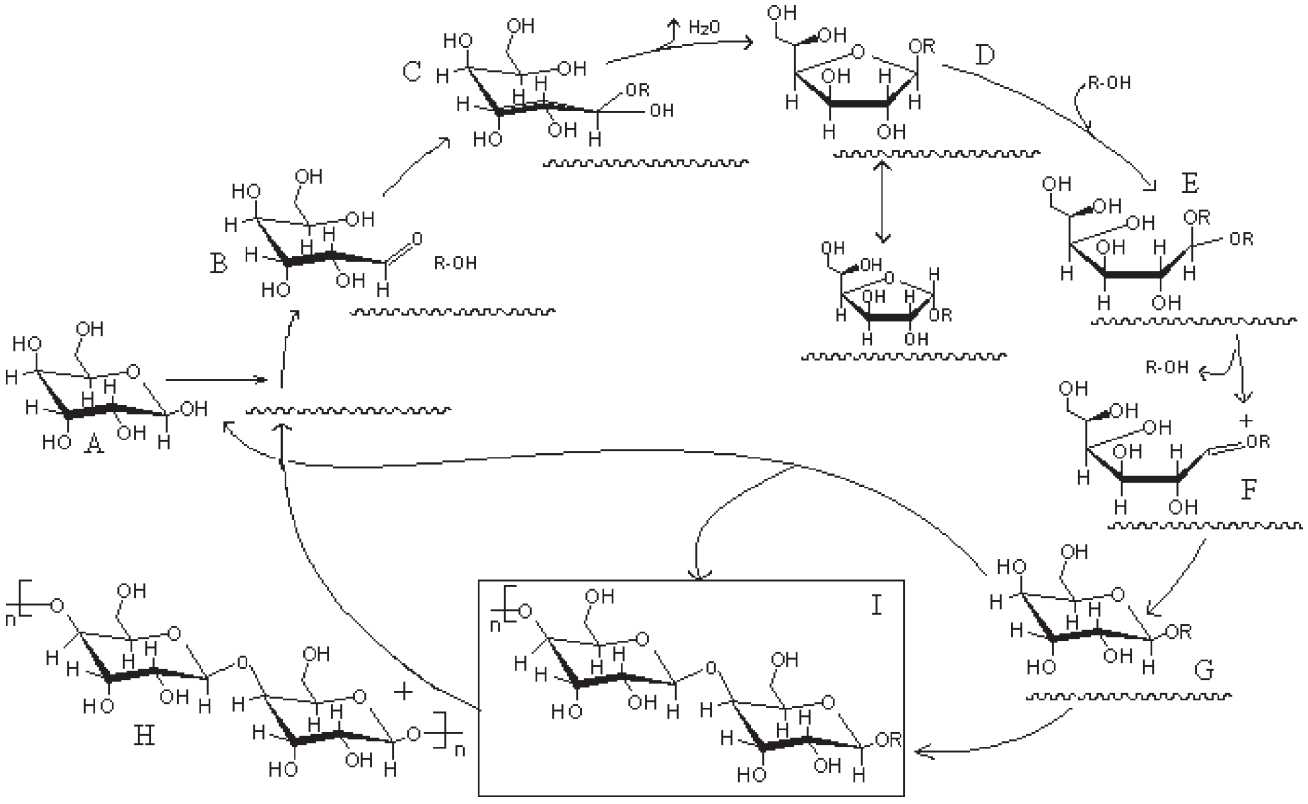

Fig. 7 – *Reaction of glucose and fatty alcohol over the surface of the $ZnFe_2O_4/ZrO_2$ catalyst to afford β-D-glucopyranoside*

furanose (D) gives alkyl poly β-D-glucopyranoside as a major product as shown in (G). The formation of alkyl poly β-D-glucopyranoside occurs due to attack of –OH of C_1 of D-glucose (A) on –OH of C_4 of alkyl β-D-glucopyranoside (G). The alkyl poly β-*D*-glucopyranoside shows inside the rectangular box. During the course of the reaction, as the catalyst surface is acidic, formation of polyglucose (H) takes place. Polyglucose formation occurs due to attack of –OH of C_1 of D-glucose (A) on –OH of C_4 of another D-glucose (A) as suggested by *Levene*, *Raymond* and *Dillon*.[16] After the formation of the product on the surface of the catalyst, desorption of the product takes place and the surface of the catalyst again starts the new reaction cycle with the adsorption of glucose and fatty alcohol.

Conclusions

The kinetics of liquid-phase glycosylation of D-glucose has been studied over a wide range of operating conditions. Zero order dependence of the initial rate with respect to the catalyst loading for the reaction was observed. The rates of glycosylation of D-glucose were zero order, with respect to the concentration of n-decanol. The experimental data could be fitted to a Langmuir-Hinshelwood type model-3, for the glycosylation reaction, involving surface reaction controlling mechanism of molecularly adsorbed n-decanol and D-glucose. The apparent activation energies for the catalytic glycosylation of D-glucose was found to be 36.75 kJ mol^{-1}.

Nomenclature

A – reactant species, D-glucose

a_p – solid-liquid interfacial area of liquid phase, m^2 m^{-3}

[Ao] – concentration of A in bulk liquid phase, kmol m^{-3}

B – reactant species, n-decanol

[Bo] – concentration of B in bulk liquid phase, kmol m^{-3}

c_A – concentration of A, mol m^{-3}

c_A – initial concentration of A in bulk liquid phase, kmol m^{-3}

c_{AS} – concentration of A at the catalyst surface, kmol m^{-3}

c_B – Concentration of B, kmol m^{-3}

c_{Bo} – initial concentration of B in bulk liquid phase, kmol m^{-3}

c_{BS} – concentration of B at the catalyst surface, kmol m^{-3}

D_{AB} – diffusion coefficient of A in B, m^2 s^{-1}

D_{BA} – diffusion coefficient of B in A, m^2 s^{-1}

d_p – diameter of the catalyst particle, m

$k_{SL\text{-}A}$ and $k_{SL\text{-}B}$ – solid-liquid mass-transfer coefficient for A and B respectively, cm s^{-1}

r_A – rate of reaction of A. kmol m^{-3} s^{-1}

r_{obs} – observed rate of the reaction, kmol kg^{-1} s^{-1}

$r_{Fe/Zn}$ – mole ratio

γ_{cat} – catalyst loading of liquid phase, kg m^{-3}

X_A – fractional conversion of A

k_1 – surface reaction rate coefficient for the glycosylation

K_B, K_C – adsorption equilibrium constants

r – initial rate of glycosylation of D-glucose, mol dm^{-3} s^{-1}

w – mass fraction, %

γ – mass concentration

ν – wave number, cm^{-1}

References

1. *Capron, B*., Chem. Rev. **69** (4) (1969) 407.
2. *Toshima, K., Ishizuka, T., Nakata, M.,* Synlett. **1995** 306.
3. *Boecker, T*., J. Tenside surf. and deter. **26** (1989) 318.
4. *Banoub, J., Bundle, D*., Can. J. Chem. **57** (1979) 2085.
5. *Paulsen, H., Paal, M*., Can. J. Chem. **53** (1984) 135.
6. *Jansson, K., Ahlfors, S., Frejd, T., Kihlberg, J., Magnusson, G., Dahmen, J., Noori, G., Stenvall, K.,* J. Org. Chem. **53** (1988) 5629.
7. *Jyojima, T., Miyamoto, N., Ogawa, Y., Matsumara, S., Toshima, K*., Tetrahedron Lett. **40** (1999) 5023.
8. *Nagai, H., Matsumura, S., Toshima, K*., Tetrahedron Lett. **43** (2002) 847.
9. *Joshi, V., Sawant, M*., Ind. J. Chem. **45** (B) (2006), 461.
10. *Chaubal, N., Sawant, M.,* J. mol. Catalysis: Chemical **267** (2006) 157.
11. *Ghorpade, S. P., Darshane, V. S., Dixit, S. G.,* Appl. Catal. A: General, **166** (1998)135.
12. *Doraiswami, L. K., Sharma*, *M. M.,* Heterogeneous Reactions: Analysis, Examples and Reactor Design, vol. 2, Wiley/Interscience, New York, 1984.
13. *Reid. R. C., Pranusnitz. M. J., Sherwood. T. K*., The properties of gas and liquids, 3rd ed.; Mc Graw-Hill; New York, 1977.
14. *Fogler. H. S.,* Elements of Chemical reaction Engineering; Prentice-Hall; New Delhi, 1995.
15. *Rode, C. V., Vaidya, M. J., Jaganathan, R., Chaudhari*, *R. V.,* Chem. Eng. Sci. **56** (2001) 1299.
16. a) *Levene, P., Raymond, A., Dillon, R.,* J. Biol. Chem. **95** (1932) 699; (b) *Smirnyagin, V., Bishop, C.,* Can. J. Chem. **46** (1968) 3085.
17. *Ferrier, R., Hatton*, *L.,* Carbohyrd. Res. **8** (1968) 56.